Journal of proteome research

ARTICLE

pubs.acs.org/jpr

Quantitative Neuroproteomics of an *In Vivo* Rodent Model of Focal Cerebral Ischemia/Reperfusion Injury Reveals a Temporal Regulation of Novel Pathophysiological Molecular Markers

Arnab Datta, Qian Jingru,[†] Tze Hsin Khor,[†] Muh Tyng Teo,[†] Klaus Heese, and Siu Kwan Sze*

School of Biological Sciences, Nanyang Technological University, 60 Nanyang Drive, Singapore 637551

Supporting Information

ABSTRACT: Cerebral ischemia or stroke, an acute neurological injury lacking an effective therapy, is the second leading cause of death globally. The unmet need in stroke research is to identify viable targets and to understand their interplay during the temporal evolution of ischemia/reperfusion (I/R) injury. Here we report a temporal signature of the ischemic hemisphere revealed by the isobaric tag for relative and absolute quantification (iTRAQ)-based 2D-LC−MS/MS strategy in an *in vivo* middle cerebral artery occlusion (MCAO) model of focal cerebral I/R injury. To recapitulate clinical stroke, two hours of MCAO was followed by 0, 4, and 24 h of reperfusion to capture ischemia with an acute and subacute durations of reperfusion injury. The subsequent iTRAQ experiment identified 2242 proteins from the ischemic hemisphere with <1.0% false discovery rate. Data mining revealed that (1) about 2.7% of detected proteins were temporally perturbed having an involvement in the energy metabolism (Pygb, Atp5b), glutamate excitotoxicity (Slc1a3, Glud1), neuro-inflammation (Tf, C3, Alb), and cerebral plasticity (Gfap, Vim, Gap43); (2) astrocytes participated actively in the neurometabolic coupling underlining the importance of a cerebro-protective rather than a neuro-protective approach; and (3) hyper-acute yet progressive opening of the blood brain barrier (BBB), accompanied by stimulation of an innate immune response and late activation of a regenerative response, which provides an extended therapeutic window for intervention. Several regulated proteins (Caskin1, Shank3, Kpnb1, Uchl1, Mtap6, Epb4.1l1, Apba1, and Ube1x) novel in the context of stroke were also discovered. In conclusion, our result supports a dynamic multitarget therapy rather than the traditional approach of a unilateral and sustained modulation of a single target to address the phasic regulation of an ischemic proteome.

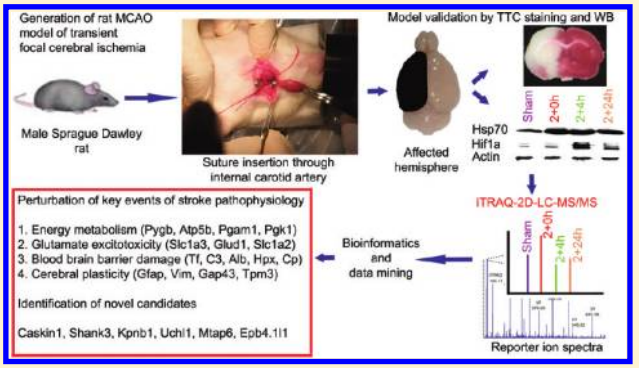

KEYWORDS: cerebral ischemia, iTRAQ, MCAO model, neuroproteomics, temporal profiling, glutamate excitotoxicity, neuro-inflammation, transferrin, stroke

INTRODUCTION

Ischemic stroke, the second most common cause of death worldwide, is a major socioeconomic burden despite decades of concerted effort to find a suitable therapy. Currently, the lone drug used in clinics, viz rt-PA (recombinant tissue plasminogen activator), is a thrombolytic agent with limited applications due to numerous exclusion criteria that include a narrow therapeutic window of around 4.5 h.[1] Hence, the pressing need in stroke research is not only the finding of realistic targets but, more importantly, the determination of the validity of these targets during the course of temporal evolution of the disease. Failure of glutamate (Glu) receptor antagonists in clinical trials was a testimony of the oversimplification of the role of Glu in the ischemic brain as well as the hyper-acute nature of Glu excitotoxicity in the pathological cascade of stroke.[2,3] In addition, a biphasic response of many proteins (e.g., vascular endothelial growth factor, Src kinase), with a transition from a pro- to an antisurvival role, or vice versa, during the evolution of the secondary injury following ischemia-reperfusion (I/R) indicates the presence of a target-specific time-window of opportunity.[2−4] Hence, a single biological marker will neither be sufficient to define this complex disease nor be conducive as a therapeutic target. Thus, to understand the dynamics of the molecular pathophysiology and to find potential therapeutic targets, a comprehensive temporal signature of the stroke-affected brain is needed. However, the traditional reductionist approach is not exhaustive enough to characterize multiple prospective targets temporally in a suitable *in vivo* model of cerebral ischemia.

Although recent advances in proteomics technologies offer opportunities to study the global protein landscape of various samples in a single experiment, neuroproteomics of cerebral ischemia still remains in its infancy.[5] Some of the earlier neuroproteomics studies on experimental ischemic brain samples would fall in the category of

Received: July 18, 2011
Published: September 27, 2011

efficacy studies,[6−8] whereas the others, that were mechanistic in nature, were either related to ischemic preconditioning[9,10] or used a longer duration of ischemia without reperfusion.[7,11] Spontaneous reperfusion following cerebral ischemia is clinically a well-documented phenomenon[12,13] that can lead to free radical injury apart from hemorrhagic complications.[14,15] Recently, postconditioning through controlled therapeutic reperfusion has gained importance in the clinical setting with the finding that uncontrolled thrombolysis can lead to reperfusion injury.[16] Thus, transient ischemia combined with an acute and subacute duration of reperfusion in a suitable *in vivo* model for temporal profiling offers better analogy to the clinical stroke, making it the strategy of choice to generate a panel of potential pathological markers or therapeutic targets by proteomics techniques.

Most of the previous studies, irrespective of their specific objectives, were technically dependent on traditional 2D-gel-based approaches (2D-GE−MS/MS).[8,9,11,17] A common subset of proteins (e.g., spectrin α II chain, heat shock proteins, and dihydropyrimidinase-related protein 2) was identified by 2D-GE−MS/MS as regulated proteins and was proposed as potential pathological markers for specific events of the ischemic pathophysiology.

In comparison with the gel-based methodologies, the LC−MS/MS-based multidimensional protein identification technology[18] combined with multiplex isobaric tag for relative and absolute quantification (iTRAQ)[19] provides an alternative approach for quantitative proteomics profiling. This sensitive technique allows the simultaneous quantification of proteins in 4- or 8-plex samples.[20] Recently, we have successfully applied the iTRAQ-2D-LC−MS/MS strategy for the first time in the area of cerebral ischemia to study a validated *in vitro* model of ischemic penumbra.[21] To extend its application into a clinically relevant *in vivo* model, we used the iTRAQ-based quantitative proteomics approach in an extra-cranial transient model of focal cerebral I/R injury for quantitative temporal profiling of the ischemic hemisphere. First, a suitable *in vivo* model of transient focal cerebral ischemia was developed. Neurological scoring of affected animals, 2,3,5-triphenyl tetrazolium chloride (TTC) staining of brain tissues and Western blots (WB) of representative hypoxia markers were performed to confirm the success of this model. Subsequently the iTRAQ-based proteomics-bioinformatics platform was applied to generate a list of the pathologically important and regulated proteome from the ischemic hemisphere. Finally, we used reverse transcription-polymerase chain reaction (RT-PCR) and WB to measure the mRNA and proteins levels of some of the perturbed candidates to better understand the source of regulation. In addition, a few of the selected proteins were spatiotemporally mapped by WB analyses to scrutinize deep into their functions during the evolution of cerebral I/R injury. Our result shows for the first time a phasic regulation of several novel proteins during the course of I/R injury thus indicating the importance of a temporally optimized therapeutic strategy to extract maximum clinical benefit.

MATERIALS AND METHODS

Reagents

Unless indicated, all reagents were purchased from Sigma-Aldrich (St. Louis, MO).

Animals

Six 8-weeks old male Sprague−Dawley rats weighing 225−275 g were cage-acclimated for 3−6 days prior to surgery in a temperature-controlled environment (24 ± 3 °C) on a 12 h light/12 h dark cycle, with food and water *ad libitum*. Animal protocols were approved by the Nanyang Technological University Institutional Animal Care and Use Committee. Before undergoing the experimental procedures, all animals were clinically normal, free of any infection or inflammation and did not show any neurological deficits.

Induction of Cerebral I/R Injury

Focal cerebral ischemia was induced by extracranial intraluminal middle cerebral artery occlusion (MCAO) following the previously described method of Zea Longa[22] with minor modifications.[23] Details of the surgical procedure are available in Materials and Methods section of the Supporting Information (SI). Briefly, the left common carotid artery, external carotid artery (ECA) and internal carotid artery (ICA) were sequentially exposed following anesthetizing the animal. A poly-L-lysine coated 30-mm length of 3−0 polyamide monofilament nonabsorbable surgical suture (Ethicon, Johnson and Johnson, Baddi, H.P, India) was inserted via ECA into the ICA until the bifurcation of left middle cerebral artery (MCA) and anterior cerebral artery to block the circulation in the left MCA territory. After 2 h of MCAO, blood flow was restored (reperfusion) by the withdrawal of the inserted suture. Sham operation was performed identically including reanesthetizing the animal after 2 h of surgery except for the brief introduction of the filament into the ECA.

Pre-Proteomics Validation

Neurological Evaluation. Postischemic motor and behavioral deficits were evaluated on a scale of 0−4 adopted from a previously reported neurological score with slight modifications.[24] Cumulative scoring (on a 10 (= 0 + 1 + 2 + 3 + 4) point scale) was performed on all animals before and after occlusion, 1 h post occlusion, before and after reperfusion to determine the success of the surgery. Details of the neurological scoring are provided in SI Materials and Methods.

TTC Staining. TTC staining was performed to confirm the presence of infarct in the MCA territory.[25] Briefly, 2 mm thick coronal sections of euthanized rat brains were placed in 1% TTC solution at 37 °C for 15 min and then fixed in buffered 4% formaldehyde solution overnight. Scion image (Alpha 4.0.3.2, Scion Corporation, Frederick, MD) was used for the calculation of the infarct area using previously published formula.[26] Details of the TTC staining procedure are provided in the SI Materials and Methods.

Proteomics

Experimental Design. The experimental design is described in Figure 1 and Table 1. All animals were randomly selected for age and body weight. The duration of MCA occlusion was fixed at 2 h to obtain reproducible infarction with lesser intergroup variation.[23,27] This 2 h MCAO model is characterized by maximum infarction and vasogenic edema during 24−48 h post-reperfusion. Thus, to evaluate the proteome regulation due to ischemia, acute and subacute phase of reperfusion injury, three groups of rats (n = 3 per group, i.e., biological replicate =3) with only 2 h of ischemia (i.e., 2 + 0 h) followed by two different lengths of reperfusion (i.e., 2 + 4 h and 2 + 24 h) were included in this experimental design. Sham surgery models of 2 h, 6 (= 2 + 4) h and 26 (= 2 + 24) h were designed to mimic the surgical trauma of 2 + 0, 2 + 4 and 2 + 24 groups respectively. The final ischemic area as a result of occlusion of MCA is rather consistent with this

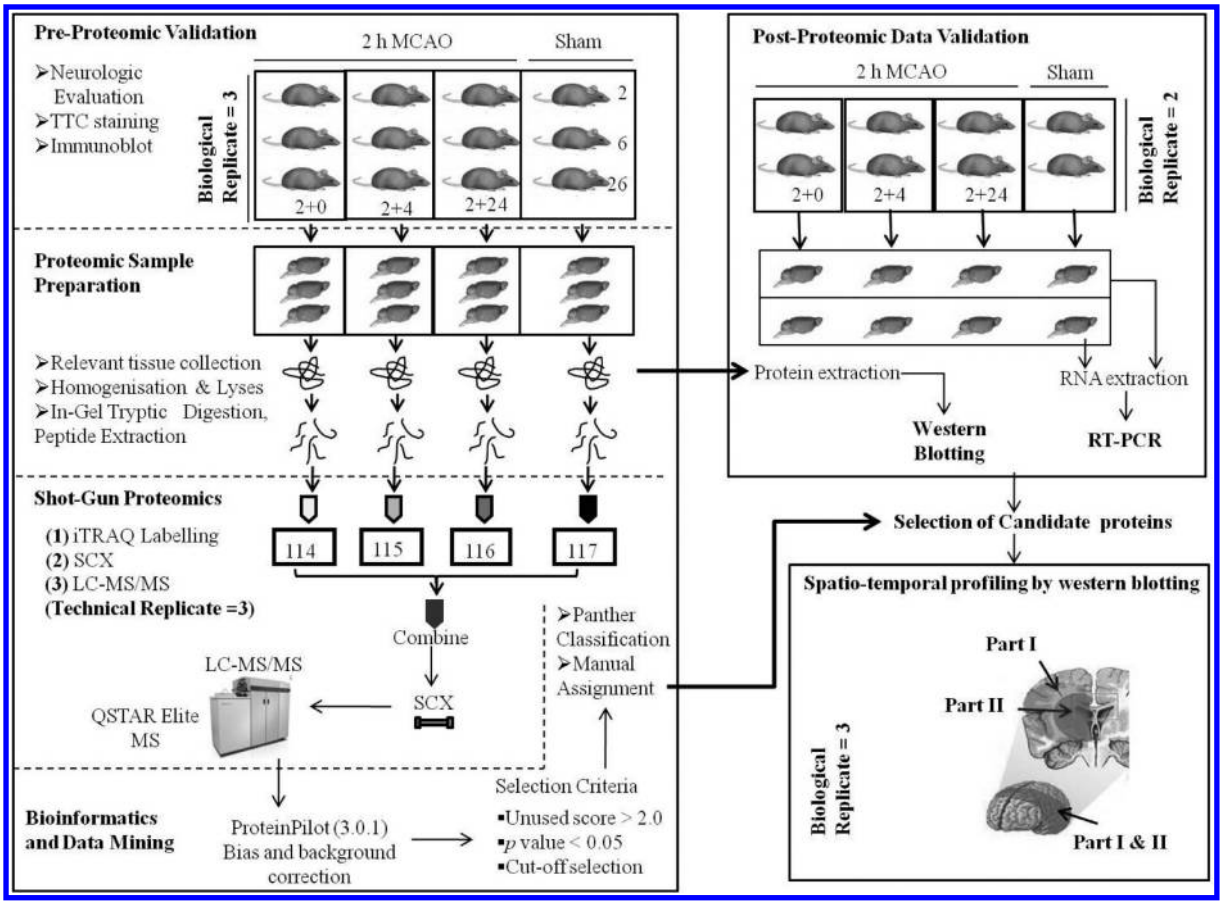

Figure 1. Schematic illustration of the experimental design classified into iTRAQ based quantitative proteomics, data verification by complementary techniques, and subsequent spatiotemporal profiling of selected candidates.

Table 1. Summary of the Group Allocation for Different Experiments

		group of animals			
experiments	purpose	sham	2 + 0 h	2 + 4 h	2 + 24 h
iTRAQ-2D-LC-MS/MS	Temporal profiling	3	3	3	3
WB	iTRAQ data Validation		Same pooled protein samples from iTRAQ experiment		
RT-PCR	Estimation of mRNA level	2	2	2	2
WB	Spatiotemporal profiling	1	3	3	3

model. But the salvageable brain tissue decreases continuously due to the expansion of injury from the core to the penumbral area during reperfusion making it difficult to select specific area of affected hemisphere for temporal profiling. Our aim was to elucidate the evolution of I/R injury as a function of time by using the quantitative proteomics strategy. Thus, the whole left or ischemic hemisphere excluding the olfactory lobe and cerebellum (hereafter called as ipsilateral hemisphere) was selected in our temporal proteomics experiment and comparison was made between groups of sham and I/R-affected animals. Moreover, pooling the ipsilateral hemisphere from three different animals minimized the surgical and biological variations between individual subjects. Injection for LC−MS/MS was performed thrice (technical replicate = 3) as multiple injections give better coverage of the target proteome with superior statistical consistency. This is especially true for single peptide proteins as more MS/MS spectral evidence was obtained from multiple injections leading to higher confidence of peptide identification and quantification.[28] The same pooled extracts were used for postproteomics data validation using WB analysis. RT-PCR was also performed in duplicate using a separate set of animals without pooling (n = 2, 4 groups). Finally, the whole hemispheric target identification strategy guided the selection of perturbed candidates for post-proteomics spatiotemporal profiling by WB analysis with three biological replicates for each group (except sham, where n = 1).

Selection Criteria. The animals showing a consistent neurological score of at least 1, 2 but not more than 3 (cumulative neurological score of 3−6) during the occlusion period were included in this study and randomly allocated between different groups. The neurological scoring was performed by the same researcher to avoid any bias in between groups. In addition, surgery duration (25 ± 5 min), completeness of perfusion and

absence of visible hematoma or hemorrhagic spot near MCA territory were also considered during selecting the animals for proteomics sample preparation to avoid intergroup variation. Details of selection criteria can be found in the SI Materials and Methods section.

Sample Preparation. The perfused ipsilateral cerebral hemispheres were obtained immediately after termination, briefly washed with PBS solution, snap-frozen in liquid nitrogen and stored at −80 °C until use. Frozen samples were homogenized with liquid nitrogen before lyses at 4 °C with ice-cold lyses buffer [2% sodium dodecyl sulfate ; 0.5 M triethylammonium bicarbonate (TEAB) with Complete Protease Inhibitor Cocktail (COMPLETE, Roche, Mannheim, Germany) and phosphatase inhibitor cocktail (PhosSTOP, Roche)] by intermittent vortexing and sonication (amplitude, 23%; pulse: 5 s/5 s for 5 min) using a Vibra Cell high intensity ultrasonic processor (Jencon Scientific Ltd., Leighton Buzzard, Bedfordshire, U.K.). The lysates were centrifuged at 20 000*g* for 30 min at 4 °C. The supernatant was collected and stored in aliquots at −80 °C (longer term) or at −20 °C (shorter duration). Protein quantification was done using Bicinchoninic Acid Protein Assay kit.

In-Gel Tryptic Digestion and Isobaric Labeling. The samples were subjected to a denaturing polyacrylamide gel electrophoresis (PAGE) for the purpose of removing the non-protein interfering substances. Briefly, 500 μg of protein from each condition were run on an 8% stacking −25% separating gel. Proteins which migrated into the 8% layer were retarded by the 25% layer, thus concentrating them in a narrow strip at the end of the stacking gel. The diced gel bands were then reduced (5 mM tris-(2-carboxyethyl) phosphine, 60 °C, 1 h) and alkylated (10 mM methyl methanethiosulfonate in isopropanol, room temperature, 15 min) before being digested with 10 ng/μL of sequencing-grade modified trypsin (Promega, Madison, WI) for overnight at 37 °C. The peptides were extracted with 50% ACN and vacuum centrifuged to dryness. The dried peptides were reconstituted into 0.5 M TEAB and ethanol, and labeled with respective isobaric tags of 4-plex iTRAQ Reagent MultiPlex kit (Applied Biosystems, Foster City, CA) as follows: sham, 114; 2 + 0, 115; 2 + 4, 116; 2 + 24, 117 (Figure 1). The labeled samples were combined after 2 h and dried in a vacuum centrifuge.

Strong Cation Exchange (SCX) Chromatography. The dried iTRAQ-labeled peptide was reconstituted in Buffer A (10 mM KH_2PO_4; 25% ACN; pH 2.85) and fractionated using a PolySULFOETHYL A SCX column (200 × 4.6 mm; 5 μm; 200 Å) (PolyLC, Columbia, MD) as mentioned previously[21] on a Prominence HPLC system (Shimadzu, Kyoto, Japan) in a 50 min gradient with Buffer B (10 mM KH_2PO_4, 25% ACN, 500 mM KCl (pH 3.0)). Eluted fractions were collected in every 1 min, and then pooled into 25 fractions, depending on the peak intensities, before drying them in a vacuum centrifuge. The dried fractions were desalted through Sep-Pak C18 SPE cartridges (Waters, Milford, MA) and stored at −20 °C until MS analysis.

LC−MS/MS Analysis using QSTAR. The iTRAQ-labeled desalted peptides were reconstituted with 0.1% formic acid (FA) for MS analysis. Each sample was analyzed three times using a QSTAR Elite Hybrid MS (Applied Biosystems/MDS-SCIEX, Foster City, CA), coupled to an online HPLC system (Shimadzu). For each analysis, 30 μL of peptide solution was injected, concentrated in a C18 peptide trap, and was separated on a home-packed nanobored C18 column with a picofrit nanospray tip (75 μm ID × 15 cm, 5 μm particles) (New Objectives, Wubrun, MA). Mobile phase A (0.1% FA in 2% ACN) and B (0.1% FA in 100% ACN) were used to establish a 90 min HPLC gradient with an effective flow rate of 0.3 μL/min, obtained from a constant flow of 30 μL/min using a splitter. The mass spectrometer was set to perform data acquisition in the positive ion mode. Precursors with a mass range of 300−1600 m/z and calculated charge of +2 to +4 were selected for fragmentation. The three most abundant peptide ions above a 5 count threshold were selected for each MS/MS spectrum. The selected precursor ion was dynamically excluded for 30 s with a 30 mDa mass tolerance. Smart information-dependent acquisition was activated with automatic collision energy and automatic MS/MS accumulation. The fragment intensity multiplier was set to 20 and maximum accumulation time was 2 s. The peak areas of the iTRAQ reporter ions reflect the relative abundance of the proteins in the samples.

Mass Spectrometric Raw Data Analysis

The spectral data acquisition was performed using the Analyst QS 2.0 software (Applied Biosystems). ProteinPilot Software 3.0, Revision Number: 114 732 (Applied Biosystems) was used for peak list generation, protein identification and quantification against the International Protein Index rat database (version 3.40; 79 354 sequences; 41 861 410 residues).[29] A concatenated target-decoy database search strategy was also employed to estimate the false discovery rate (FDR). FDR was obtained by calculating the percentage of decoy matches among total matches. The user defined parameters of the software were configured as described previously with minor modifications (ID Focus: biological modification). The Proteinpilot software employed Paragon and Pro Group algorithm for the peptide identification and isoform-specific quantification respectively. Details of the quantification algorithm can be found in the supplier's manual. The resulting data set were auto bias-corrected to get rid of any variations imparted due to the unequal mixing during combining different labeled samples. Subsequently background correction was also performed to eliminate any background ion signal due to nontarget peptides, coeluting with the target peptide.

Bioinformatics Analysis

Batch search was adopted by uploading the gene IDs of the proteins of interest using PANTHER 7.0 (Protein Analysis Through Evolutionary Relationships) classification system[30] against the NCBI (*Rattus norvegicus*) data set. The regulated genes were categorized according to the molecular functions or biological processes or protein classes or pathways.

WB Analyses

WB was performed after SDS-PAGE by probing with specific horseradish peroxidase (HRP)-conjugated primary antibodies directed against proteins at the indicated dilutions: hypoxia-inducible factor-1 (Hif1a) (clone H1alpha67, 1:500; Novus Biologicals, Littleton, CO), Tf (1:2000, Abcam Ltd., Cambridge, UK), heat shock protein 70 (Hsp70, 1:5000; Abcam Ltd.), Slc1a3 (1:1000; Cell Signaling, Danvers, MA), Caskin1 (1:1200; Santa Cruz Biotech, Santa Cruz, CA), Vcl (1:4000; Millipore, Billerica, MA), Vim (1:2000; Millipore), Gfap (1:10 000; Millipore), Actn1 (clone C4, 1:4000; Millipore), β-tubulin (clone B7, 1:2500; Santa Cruz). Immunoreactivity was detected by using an HRP chemiluminescent substrate reagent kit (Invitrogen, Carlsbad, CA). The membranes were stained with Ponceau S and

Table 2. Regulation of Physiological Variables during the Course of Cerebral I/R Injury in Sprague Dawley Rats[a]

		groups	
physiologic parameter	condition	2 + 4 h	2 + 24 h
% Decrease in Weight (g)	Surgery	3.7 ± 1.6	11.8 ± 2.5
	Sham	1.5 ± 0.4	5.2 ± 1.8

		0 h	2 + 0 h	2 + 4 h	2 + 24 h
Temp (°C)	Surgery	37.1 ± 0.4	38.8 ± 0.5	38.6 ± 0.4	38.2 ± 0.6
	Sham	37.2 ± 0.3	37.2 ± 0.6	37.5 ± 0.3	37.4 ± 0.6

[a] Data was presented as mean ± SD ($n \geq 6$, surgery; $n \geq 3$, sham). Body weight at 0 h postreperfusion and preoperative rectal temperature (0 h) were used as respective controls for the statistical test (one way ANOVA followed by Dunnett's Multiple Comparison Test). Significant increase in % loss of body weight and rectal temperature was observed following the MCAO model of cerebral I/R injury in comparison to the sham group of animals.

later stripped and reprobed against the Actn1 or β-tubulin antibody to confirm uniform transfer and equal loading.

RNA Isolation and RT-PCR

Specific primers were designed by using open-source primer 3.0 software for C3, Gfap, Caskin1, Nefl, Tpm3, and Actn1 (Supplemental Table 1, SI). Total RNA was isolated using TRIzol reagent (Invitrogen) according to the manufacturer's protocol and quantified in μg/μL. Two μg of RNA was used for the RT reaction with the RevertAid H Minus Moloney Murine Leukemia Virus Reverse Transcriptase kit (Fermentas Life Sciences, Hanover, MD) following the manufacturer's instructions. Actn1 was used as internal control to check the efficiency of cDNA synthesis, PCR amplification and uniform loading. PCR products were electrophoresed through 1% agarose gels.

Spatiotemporal Profiling by WB Analyses

In the MCAO model, subcortical regions (preoptic area and striatum) are first and more severely affected as a result of microvascular injury with higher chances of blood brain barrier (BBB) damage-induced edema and hemorrhagic transformation.[31] Conversely, the cortex in the transient MCAO model is affected in the later stage, thus making it suitable to study the spatial trend of the secondary injury.[12] Hence, 6 mm coronal section of the ipsilateral hemisphere starting 7 mm caudal to the frontal lobe was divided into two parts; the cortical (part I) containing somatosensory cortex and the subcortical (part II), containing caudoputamen or striatum, to understand the spatiotemporal pattern of the selected proteins from the temporal proteomics experiment. The dissection was guided by the knowledge of the vascular architecture of the rat brain and by the TTC staining done during the model development and was based on the reports on the evolution of the infarct in this MCAO model.[12,32]

Statistical Analysis

The physiologic variables (e.g., temperature, body weight) were presented as mean ± standard deviation (SD) to report the variability of the observations. The ordinal variable (i.e., cumulative neurological score) was presented as median ± SD. The n value indicated the number of replicate readings from same or different experiments. The possible correlation between nonparametric variables was determined using Spearman rank correlation coefficient (time vs cumulative neurological score). One-way ANOVA followed by post hoc Dunnett's multiple comparison test or nonparametric Kruskal–Wallis test followed by chi-square test was performed for comparing scale (physiological variables) or ordinal variables (neurological score) respectively involving at least three groups. Statistical significance was accepted at $^{*}p < 0.05$ and $^{**}p < 0.01$, respectively.

RESULTS

Preproteomics Validation of the *In Vivo* Model of Focal Cerebral Ischemia

Physiological Monitoring. Rectal temperature and body weight were monitored at periodic intervals until the sacrifice of the animals. There was a statistically significant increase in weight loss at 24 h postreperfusion for stroke affected rats (11.8 ± 2.5%) in comparison with sham rats (5.2 ± 1.8%) (Table 2, Supplemental Figure 1A, SI) due to the combined insult of intracranial and extracranial ECA territory ischemia, although the brain edema or final lesion size due to MCAO was not affected by this extracerebral ischemia.[33] Hyperthermia was observed in all the groups except sham due to the hypothalamic ischemia that peaked (38.8 ± 0.5 °C) at the end of 2 h of occlusion and persisted until 24 h postreperfusion (38.2 ± 0.6 °C) (Table 2, Supplemental Figure 1B, SI).[35] Detailed results are presented in the SI Results section.

Neurological Deficits and Mortality. Neurological deficit peaked at the end of 2 h of MCAO (6.0 ± 1.3), whereas progressive and partial recovery was observed spontaneously after reperfusion that persisted until 24 h (Supplemental Figure 2, SI). This may be partly because of the use of young adult rats, a situation also encountered for younger human population with ischemic stroke.[13]

Postoperative mortality was around 3.6% due to subarachnoid hemorrhage, whereas another around 18.2% was excluded due to an insufficient neurological score during the course of occlusion and early reperfusion or due to the presence of a hemorrhagic spot at the base of the autopsied brain. Thus, around 78% of the total population was progressed into the next phase for the molecular validation. Detailed results can be found in the SI Results section.

TTC Staining. The terminal TTC staining was performed for all four groups as part of a preproteomics model validation that indicated massive infarction in the striatum and the overlying cortex after 24 h of reperfusion (Figure 2, Supplemental Figure 3, SI). The overall corrected % hemispheric infarction area (% HIA) was found to be around 35% which is similar to the previously published reports.[27] The ipsilateral hemisphere at the level of bregma was the most affected one, where around 74% of the area became necrotic by 24 h of reperfusion. Hypothalamic ischemia

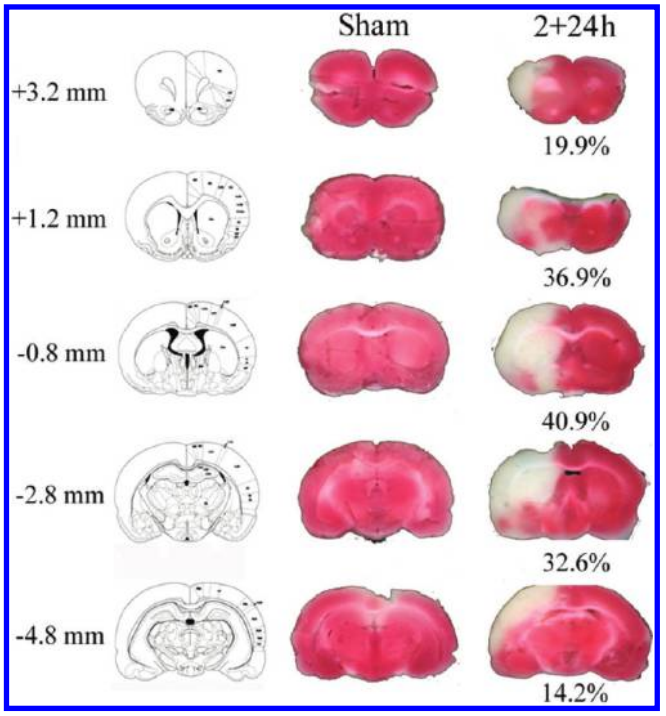

Figure 2. TTC staining of the representative coronal sections from sham and 2 + 24 group with a corresponding schematic diagram and respective anterio-posterior position to bregma (0 mm). White indicates infarction; red indicates normal tissue. Infarct area was maximum at the level of bregma (% HIA is 74% at 0.8 mm posterior to bregma) after 24 h of I/R injury. No ischemic lesion was observed in the sham group.

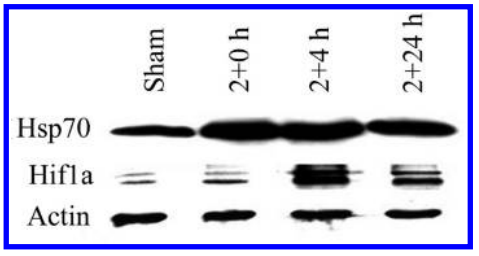

Figure 3. Molecular validation of the rat MCAO model of I/R injury by WB analysis. Pooled lysate from each group were probed with monoclonal antibodies against Hsp70 and Hif1a along with actin as loading control. Hsp70 expression was high until 24 h of I/R injury, whereas expression of Hif1a peaked at 4 h postreperfusion.

was also apparent in the 2 + 24 group as a result of 2 h of MCAO, as reported previously.[27]

Molecular Validation by WB Analyses. Hif1a and Hsp70 were selected as representative pathological markers for completing the validation process of our rat MCAO model at the molecular level.[34] The antiapoptotic stress protein Hsp70 is generally regarded as an early response chaperone and a marker of metabolic deprivation in cerebral ischemia that increases the expression of many downstream proteins as a part of the survival response.[35] In contrast, the transcription factor, Hif1a is induced following a reduction in oxygen supply but not due to the inhibition of mitochondrial respiration and it controls the glycolysis and angiogenesis in the ischemic brain.[35] During the entire 26 h (2 + 24 h) of I/R experiment the increased expression

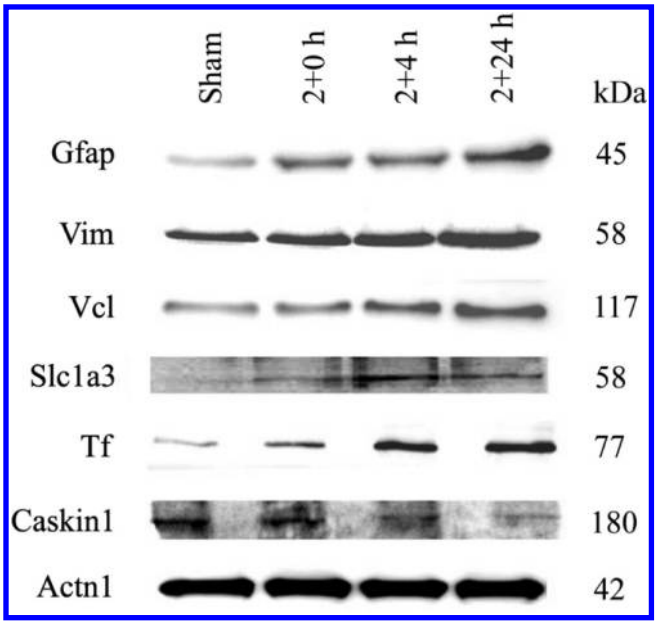

Figure 4. Postproteomics validation of the selected proteins by WB analysis using the same pooled extract from the iTRAQ experiment. Cytoskeletal proteins (Gfap, Vim, Vcl) and Tf peaked 24 h after I/R injury. Slc1a3 expression was highest at 4 h postreperfusion while Caskin1 showed a gradual decline until 24 h postreperfusion. Actn1 was used as loading control. All of them showed consistent trends with the iTRAQ results.

of Hsp70 and the transient up-regulation of Hif1a (with a peak at 4 h of reperfusion) compared with the sham hemisphere (Figure 3) indicated the specific stress response by the viable cells confirming the success of our rat I/R model.

Proteomics

Group allocation for the proteomics and spatiotemporal profiling experiments were finalized after carefully screening the animals to comply with the selection criteria as mentioned previously. The groups were similar ($p > 0.05$, one way ANOVA) with respect to the measurable parameters like preoperative body weight or rectal temperature (Supplemental Table 2, SI) and pre- or postischemic cumulative neurological score (data not shown).

iTRAQ Results. To understand the global proteomics changes that occurred in the ipsilateral hemisphere at different time-points, pooled protein extracts from each group ($n = 3$, biological replicate) were labeled and analyzed thrice (technical replicate =3) as described in the experimental procedure. Details of the replicates are provided in the Supplemental Data A and B (SI). The ProteinPilot software-generated protein and peptide summary of the combined data set are provided in the Supplemental Data C and D (SI).

Quality Control of iTRAQ Data set. To minimize the false positive identification of proteins, a strict cutoff of unused ProtScore ≥2 was used as the qualification criteria, which corresponds to a peptide confidence level of 99%. With this criterion, 2242 proteins were identified with a FDR of 0.33% (Supplemental Data A and C, SI). The average number of unique peptides (having a confidence level of >95%) detected per protein was 9.23 and 37% of the proteins had ≥5 unique peptides which was similar to our recently published report (Supplemental Data C).[21] The ratios for each condition were sorted using a p-value cutoff of 0.05 to obtain the list of proteins with significant ratios.

Table 3. Quantitative Information of the Significantly Regulated Proteins Obtained from the Bias and Background Corrected iTRAQ Data Set Showing a Temporal Pattern in the Transient MCAO Model of Cerebral I/R Injury[a]

N	unused	%cov (95)	gene symbol	protein name	unique peptides (95%)	total peptides (95%)	115:114 (2 + 0:sham)	116:114 (2 + 4:sham)	117:114 (2 + 24:sham)
				Energy metabolism					
29	65.7	41.6	Pygb	brain glycogen phosphorylase	47	154	**3.08**	1.60	2.73
38	60.5	53.5	Atp5b	ATP synthase subunit beta, mitochondrial precursor	83	414	**3.63**	**3.37**	**3.53**
48	58.5	31.4	Hk1	Hexokinase-1[d]	50	220	1.36	0.85	1.43
56	54.5	44.7	Atp5a1	ATP synthase subunit alpha, mitochondrial precursor	67	463	**2.42**	1.84	1.84
65	49.4	43.4	LOC688509	similar to Alpha-enolase	50	159	1.39	1.47	**1.72**
91	42.5	36.0	Ndufs1	NADH-ubiquinone oxidoreductase 75 kDa subunit, mitochondrial precursor[d]	31	87	1.46	1.21	1.71
119	38.0	49.2	Pgk1	Phosphoglycerate kinase 1	34	176	**2.56**	**2.36**	**2.56**
179	29.0	26.2	Pygm	Glycogen phosphorylase, muscle form[d]	23	50	1.33	0.97	1.11
216	25.6	60.2	Tpi1	Triosephosphate isomerase	20	50	**1.58**	1.37	**1.38**
333	18.8	28.5	Ndufs2	NADH dehydrogenase (Ubiquinone) Fe−S protein 2[d]	10	22	1.27	1.33	1.15
357	17.7	37.0	Pgam1	Phosphoglycerate mutase 1	11	38	**2.56**	1.53	**1.84**
				Glutamate excitotoxicity					
8	169.6	47.1	Cltc	Clathrin heavy chain	177	804	1.02	**1.94**	1.41
115	38.8	41.8	Glud1	Glutamate dehydrogenase 1, mitochondrial precursor	27	67	**4.25**	2.42	2.56
120	37.9	21.4	Slc1a2	Isoform Glt-1A of Excitatory amino acid transporter 2[d]	39	289	1.10	1.82	1.28
152	31.8	36.5	Glul	Glutamine synthetase[d]	30	87	1.80	1.84	1.85
243	24.0	21.9	Slc1a3	Isoform GLAST-1 of Excitatory amino acid transporter 1 (EAAT1)[b]	31	168	1.36	**1.64**	1.18
1387	4.0	6.5	Slc16a1	Monocarboxylate transporter 1 (MCT1)[d]	3	7	1.39	1.58	1.37
2070	2.0	4.8	Slc1a1	Excitatory amino acid transporter 3[d]	2	3	0.86	0.79	0.91
				Neuro-inflammation and iron metabolism					
42	60.1	54.9	Alb	Serum albumin precursor	45	176	2.21	**18.20**	**24.89**
131	36.8	29.7	Tf	Isoform 1 of Serotransferrin precursor[b,c]	23	125	2.09	**6.25**	**9.55**
458	14.2	58.5	Hbb	Hemoglobin subunit beta-1	9	28	**3.47**	**2.96**	1.69
491	13.5	5.1	C3	Complement C3 precursor (Fragment)[c]	6	16	1.08	**7.59**	**7.18**
619	10.5	6.5	Cp	121 kDa protein	5	11	0.85	**2.54**	**4.13**
734	8.7	4.3	Pzp	Pregnancy-zone protein, 167 kDa protein	4	7	0.73	**7.31**	**6.49**
978	6.1	6.7	Hpx	Hemopexin precursor	3	4	1.63	**3.47**	**5.20**
1217	4.5	5.3	Fetub	Fetub protein	2	2	3.60	**7.59**	**14.59**
1242	4.3	5.7	Mug1	Isoform 1 of Murinoglobulin-1 precursor	7	14	1.04	**6.55**	**6.67**
2239	2.0	16.3	S100b	Protein S100−B[d]	3	37	1.45	2.05	2.10
				Cerebral plasticity					
Synapse related proteins									
81	44.5	39.0	Mtap6	STOP protein	25	72	0.69	**0.45**	**0.51**
84	43.6	18.4	Epb4.1l1	Isoform L of Band 4.1-like protein 1	36	94	0.77	0.74	**0.55**
133	36.0	19.4	Caskin1	Caskin1[b,c]	22	44	0.61	**0.59**	**0.48**
155	31.4	13.1	Shank3	Isoform 1 of SH3 and multiple ankyrin repeat domains protein 3	15	36	0.81	0.94	**0.57**
269	22.4	11.4	Ctnnd2	similar to Catenin delta-2	11	31	0.82	**0.69**	**0.66**
974	6.1	5.7	Apba1	Amyloid beta A4 precursor protein-binding family A member 1	4	7	0.70	0.73	**0.59**

dx.doi.org/10.1021/pr200673y |J. Proteome Res. 2011, 10, 5199–5213

Table 3. Continued

N	unused	%cov (95)	gene symbol	protein name	unique peptides (95%)	total peptides (95%)	115:114 (2 + 0:sham)	116:114 (2 + 4:sham)	117:114 (2 + 24:sham)
Structural proteins									
1	396.7	63.2	Spna2	Spectrin alpha chain, brain	405	1957	**0.83**	1.15	1.43
2	287.7	36.7	Dync1h1	Dynein heavy chain, cytosolic	207	706	**0.64**	0.90	1.01
4	198.5	28.6	Plec1	Plectin 3	105	273	**0.56**	**0.96**	1.19
6	175.6	45.3	Spnb3	Spectrin beta chain, brain 2	142	524	**0.65**	0.88	0.94
7	173.8	42.0	Mtap1a	Microtubule-associated protein 1A	122	396	**0.94**	**0.63**	**0.94**
11	153.1	42.6	Myh10	Myosin-10	105	321	**0.57**	**0.77**	1.39
111	39.3	46.1	Nefl	Neurofilament light polypeptide[c]	39	127	**1.94**	1.04	**1.87**
141	33.4	47.7	Gfap	Isoform 1 of Glial fibrillary acidic protein[b,c]	27	92	1.15	0.88	**1.66**
185	28.3	16.9	Vcl	vinculin[b]	15	43	0.84	1.25	**1.56**
186	27.8	37.5	Vim	Vimentin[b]	19	60	1.10	0.79	**1.66**
238	24.3	42.0	Gap43	Neuromodulin	22	48	**5.97**	**3.77**	**5.01**
403	15.8	25.4	Tpm3	Isoform 1 of Tropomyosin alpha-3 chain[c]	8	18	**2.99**	**2.99**	**3.22**
				Ubiquitin proteosome system					
44	59.1	34.1	Ube1x	Ubiquitin-activating enzyme E1, Chr X	56	228	1.39	1.02	**1.74**
599	10.9	31.4	Uchl1	Ubiquitin carboxyl-terminal hydrolase isozyme L1	9	15	**2.81**	**1.85**	**1.77**
				Nucleocytoplasmic transport					
169	30.01	22.03	Kpnb1	Importin subunit beta-1	16	44	**1.33**	1.18	**1.50**
197	27.07	17.4	Ipo7	predicted importin 7[d]	13	54	1.13	0.95	1.34
				Housekeeping gene (control for WB, RT-PCR)					
40	60.09	39.9	Actn1	Brain-specific alpha actinin 1 isoform[b,c]	37	136	1.02	0.98	1.05

[a] Most of these proteins have qualified through the preset selection criteria (i.e., unused prot score > 2.0, p-value <0.05 for at least one ratio, magnitude of expression changes of at least 1.4 fold compared to the sham group), as mentioned in the "Results" section. They were classified according to their participation in the key molecular events of stroke pathophysiology. The ratios with significant p-value (<0.05) are shown in **bold**. [b] Proteins validated by WB. [c] Proteins whose of transcripts were measured by RT-PCR. [d] Proteins incorporated in the list due to their close association with the regulated proteins although they did not meet the above-mentioned preset selection criteria (i.e., unused prot score >2.0 but p-value >0.05). For example, Hk1, Ndufs1 and Ndufs2 (energy metabolism) are important enzymes of glucose catabolism. Pygm was the unperturbed muscle isoform of glycogen phosphorylase, whose brain isoform was significantly upregulated after 2 h MCAO. Similarly, Slc1a2, Glul, Slc16a1, Slc1a1 are related to Glu neurotransmission and metabolism.

Estimation of Cutoff for Confidently Defining Perturbed Proteins. Next, the cutoff for up- or down-regulation was determined based on the analytical variation between three technical replicates (Supplemental Figure 4).[21] Details of the process can be found in the SI Results section. The regulation cutoff was set at 1.4 fold; ratio >1.40 or <0.71 was considered as up- or down-regulated. Subsequently, the final list of regulated candidates was obtained separately for each time-point by applying the p-value and regulation cutoff. Thus, 24, 28, and 37 proteins from 2 + 0, 2 + 4 and 2 + 24 group (having overlap between different time-points) respectively showed significant perturbation with a magnitude beyond the specified cutoff of 1.4 fold. Combining all time points, only 61 candidates (2.72% of total hits) remained having at least one significant ratio ($p < 0.05$) with the expression level >1.40 or <0.71 (Supplemental Table 3A, SI). This data set was advanced to the next phase for rigorous validation by complementary techniques.

Postproteomics WB and RT-PCR of Selected Proteins

Six proteins (i.e., Tf, Slc1a3, Caskin1, Vim, Vcl and Gfap) out of 61 candidates representing distinct events in the pathology of ischemic stroke were chosen from the data set. Tf is a circulatory protein whereas Slc1a3 (excitatory amino acid transporter) is an astrocyte-specific membrane-bound high-affinity sodium-dependent aspartate/Glu transporter. Three intermediate filament-related structural proteins (Gfap, Vim and Vcl) were chosen as they may be representative of the neurorestorative response in the ischemic brain. As seen in Figure 4 and Table 3, WB showed similar trends with the corresponding iTRAQ ratios.

In addition, RT-PCR of five genes selected from the list of perturbed proteins ((C3, Caskin1, Gfap (Figure 5) and Tpm3, Nefl (Supplemental Figure 5, SI)) showed similar trends to the iTRAQ results.

Temporal Regulation of Perturbed Proteins following Focal Cerebral I/R Injury

The gene IDs of the significantly regulated proteins from the filtered and validated data set were classified by PANTHER 7.0 using "pathway" as ontology. Most of the genes were assigned to more than one category thus making the total number of hits greater than the number of genes uploaded. They were assigned to 18 different pathways (Supplemental Table 4, SI). Among

total pathway hits, 14.2% and 14.3% of the gene hits were associated with glucose metabolism (7.1% each for ATP synthesis and glycolysis) and Glu neurotransmission (7.1% for the ionotropic Glu receptor pathway and 3.6% each for the metabotropic Glu receptor group III pathway and glutamine/Glu conversion) respectively. Blood coagulation (14.3%), inflammation (3.6%) and angiogenesis (3.6%) were featured among the other perturbed pathways that were consistent with the vascular nature of this disorder. Strikingly, a few of the regulated genes (Uchl1, Apba1, Dync1h1) were also assigned to various chronic neurodegenerative disorders (e.g., Parkinson's disease, Alzheimer's disease (AD) and Huntington's disease). Guided by the above trends, regulated proteins were manually classified (Table 3) with incorporation of additional candidates based on their identification information only (Supplemental Table 3B, SI) considering their association with the regulated proteins (see Discussion).

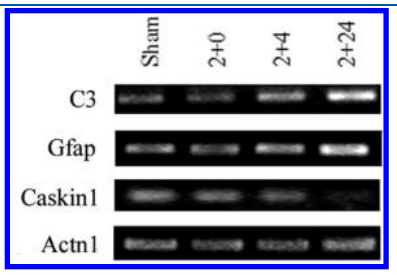

Figure 5. Representative RT-PCR images of the selected genes at identical time-points as the iTRAQ experiment. C3 showed an increasing trend from 4 h onward whereas Gfap exhibited a late up-regulation after 24 h of reperfusion injury. In contrast, Caskin1 was down-regulated at 24 h postreperfusion.

Sustained up-regulation of energy metabolism related proteins following I/R injury signified an adaptive response of the stressed brain that includes glycogen mobilization (i.e., Pygb) to glycolysis (e.g., Pgk1, Pgam1) and the oxidative phosphorylation (e.g., Atp5b, Atp5a1) (Figure 6A, B). Early up-regulation was seen for two glial Glu transporters (Slc1a3 and Slc1a2) having a neuroprotective role in the Glu-mediated excitotoxicity.[36] Persistent increase in Glul, an enzyme with almost exclusive astrocytic localization, and significant up-regulation of Glud1 were observed after 2 h of ischemia. Considering I/R injury as a combination of the hypoxic and metabolic stress, active involvement of sirtuins could be possible as an upstream modulator of the deregulated Hif1a and Glud1 in this current model.[37,38] Accordingly, two isoforms of sirtuins (Sirt2 and Sirt5) were identified in our data set (Supplemental Table 3B, SI) whose expression is reported to be higher in the adult brain relative to the fetal brain unlike other isoforms of sirtuins, thus supporting the above assumption.[39]

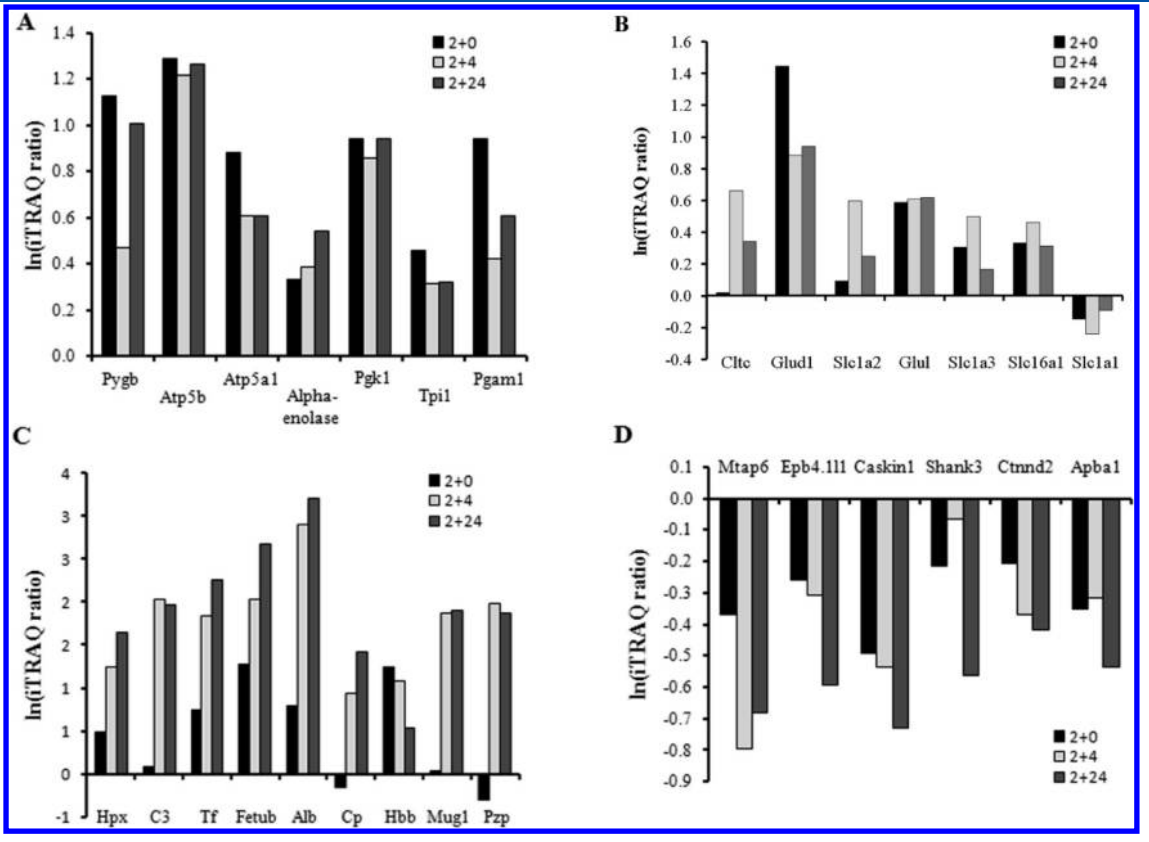

Figure 6. Histograms showing the relative temporal expression patterns of regulated proteins in the ischemic hemisphere during the course of cerebral I/R injury. Natural logarithm of iTRAQ ratios of the proteins with respect to sham group were plotted on the vertical axis. The gene symbols were plotted on the horizontal axis. (A) Proteins related to glycolysis and glycogen mobilization showed a persistent up-regulation. (B) Proteins taking part in the Glu excitotoxicity were mostly up-regulated especially after 4 h of reperfusion except the neuronal subtype of Glu transporter, Slc1al that showed a downward trend. (C) Increasing trend of all circulatory proteins (except Hbb) signified a gradual leakage of the BBB causing progressive vasogenic edema. (D) The synapse related proteins (Mtap6, Epb41l1, Caskin1, Shank3, Ctnnd2, and Apba1) exhibited a generalized downward trend implying the compromised synaptic function. Notably all of them were novel in the pathology of cerebral ischemia.

dx.doi.org/10.1021/pr200673y |J. Proteome Res. 2011, 10, 5199–5213

The significant presence of several acute phase proteins in the brain parenchyma after 2 h of ischemia (Figure 6C) indicated a hyper-acute opening of the BBB as reported recently.[40] All candidates of this group except Hbb (beta-1 subunit of hemoglobin) showed an ascending trend of absolute expression signifying a progressive neuro-inflammation and vasogenic edema as a result of the I/R injury. The precipitous elevation in the overall expression of albumin can be explained by the complementary *de novo* expression in the ischemic hemisphere when albumin mRNA and protein expression was elevated after 2 h of MCAO and 22 h postreperfusion.[41] To evaluate the *de novo* component on the overall expression of the plasma-derived candidates, C3 was chosen as a representative and its expression level was checked at the transcript level. Gradual increase in the mRNA level of C3 after 24 h (Figure 5) indicated the participation of brain cells in complement generation that is most likely supplemented by the massive infiltration of circulatory leukocytes and direct leakage of C3 from the circulation.

A significant decrease in the levels of essential structural and cytoskeletal proteins (e.g., Myh10, Plec1, Dync1h1, and Spnb3) was observed 2 h after MCAO that was probably related to an irreversible activation of intracellular proteases (Table 3). All of them recovered while some others showed significantly increased levels (e.g., Gap43, Gfap, Vim, Vcl, Nefl, and Tpm3) at the end of 24 h of reperfusion indicating the presence of cerebral plasticity in the ischemic brain. This may be a part of the endogenous recovery response happening in parallel with the worsening of the secondary injury as exhibited by the generalized downward trend of the synapse related proteins (e.g., Mtap6, Caskin1, Ctnnd2), the other subclass under the category of "cerebral plasticity" (Figure 6D). These contradictory trends of the growth-promoting (e.g., Gap43, Gfap or Vim) and synaptic proteins (e.g., Mtap6, Caskin1, Shank3) can be attributed to the heterogeneity of the brain substructures or to the differential cellular or subcellular origin of the candidate proteins. Detailed immunohistochemical studies are needed to elucidate the underlying molecular complexities.

The regulated list also consists of several proteins (e.g., Caskin1, Shank3, Apba1, Ctnnd2, Ube1x, Kpnb1) novel in context of the pathophysiology of cerebral ischemia highlighting the utility of this discovery approach. Hence, the individual proteins can further be explored through functional studies in similar animal or simpler cell-line models.

Spatiotemporal Profiling of the Validated Candidates

Two of the validated candidates (Tf and Gfap) from the iTRAQ data set, representing two distinct events of stroke pathophysiology (Table 3) were chosen to define this model by spatiotemporal profiling. As seen from Figure 7, the presence of Tf peaked at 4 h in the striatum (I) followed by a plateau or decrease at 24 h, whereas in the overlying cortex (II), a gradual but detectable increase with time was observed as inflammation and vasogenic edema spread into the ischemic area. The well studied astrocytic marker, Gfap showed a late up-regulation in part I and recovered from an early decrease in the part II at 24 h post I/R injury, indicating the presence of reactive gliosis in the MCA territory.

DISCUSSION

We report an overview of the perturbation of ischemic proteome in the first 24 h of cerebral I/R injury showing the deregulation of fundamental mechanisms (failure of energy metabolism, Glu excitotoxicity, and inflammation) that orchestrate the cell death following ischemic stroke. Most of the potential therapeutic interventions tried to target one or more of these deleterious events without a single clinical success. Recent evidence indicated that each of these mechanisms may have some neurorestorative role at some point of time during the evolution of cerebral I/R injury.[2,3] Thus temporal considerations are important as terminating the therapy in time may be equally important as its well-timed initiation to extract maximum clinical advantage. Further, understanding the underlying molecular mechanisms and evaluating the efficacy of the therapy will remain a serious challenge in absence of any standard diagnostic protocol to demarcate and measure the ischemic penumbra, core and the normal tissue as they usually remain scattered and highly heterogeneous.[42,43] Animal models of stroke are more uniform and can be controlled precisely to represent specific types of human stroke. MCA, being one of the most common sites of human large artery stroke, makes transient MCAO, a clinically relevant and the most widely accepted rodent model for understanding the temporal complexities of the cerebral I/R injury.[4]

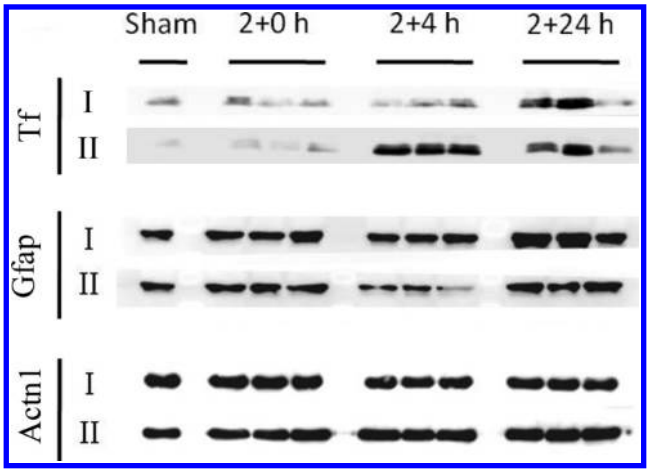

Figure 7. Spatiotemporal profiling of the validated candidates (Tf and Gfap) by WB analysis in the striatum (part II) and in the overlying cortex (part I) of the ipsilateral hemisphere. Actn1 was used as loading control. Each time point has three biological replicates except sham. Early opening of the BBB was evident by the leakage of circulatory Tf at 4 h postreperfusion in the striatum. Gfap showed a reverse trend in the striatum at the same time signifying the astrocytic damage. Elevation of the Gfap level in both parts after 24 h of I/R injury was indicative of the reactive gliosis, constituting a recovery response.

Unraveling the Temporal Evolution of Ischemic Pathophysiology in the transient MCAO model by Analysis of the iTRAQ Data set

The final list of regulated proteins (Table 3) was functionally analyzed to interpret the molecular events relevant to the pathophysiology of cerebral ischemia in a chronological way.

Alteration of Energy Metabolism and Glu Excitotoxicity—Neuron-Astrocyte Cross-talk

Focal ischemia is associated with an acute release of a massive amount of Glu by the glutaminergic synapses that represent >85% of the cortical synapses.[44] In neurons, Glud1 plays an essential role in generating releasable Glu stored in the synaptic vesicles. Increased *in vivo* release of Glu has been observed after neuronal depolarization in transgenic mice overexpressing Glud1.[45] Thus, significant up-regulation of Glud1 following 2 h of MCAO indicated the excitotoxic release of Glu in the ischemic brain by the depolarized neurons. The excess Glu in the synaptic

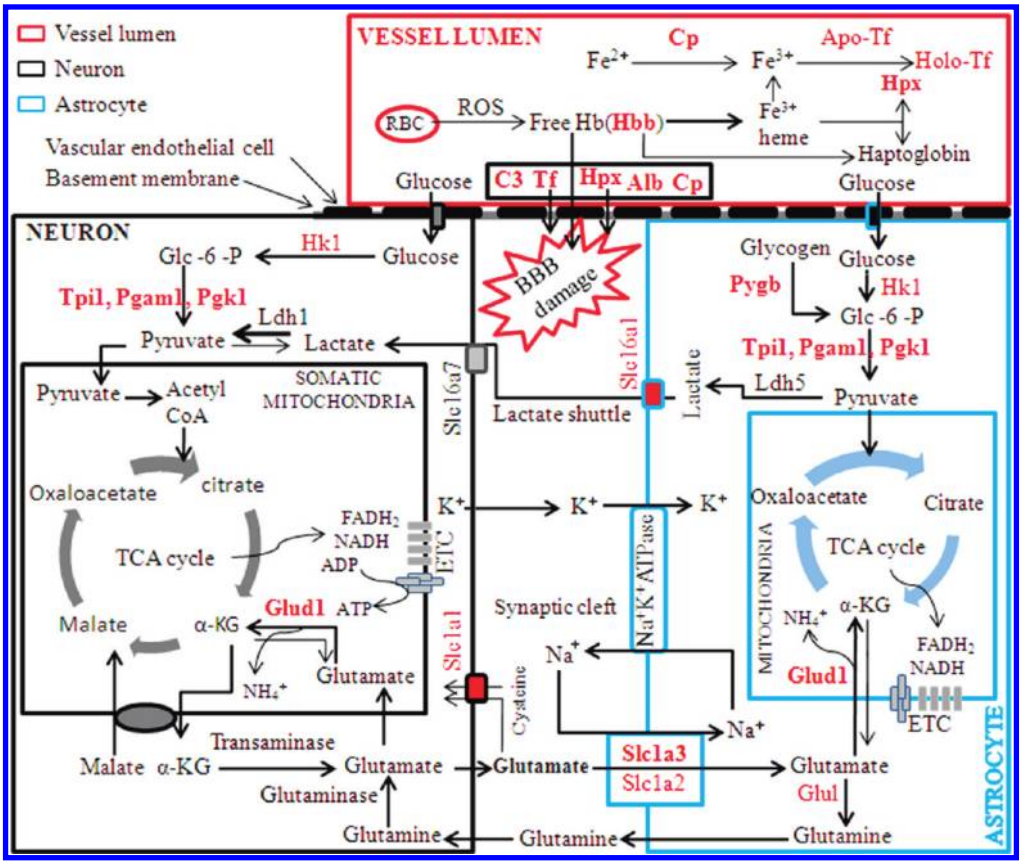

Figure 8. Schematic diagram showing the interplay of glucose metabolism, Glu excitotoxicity, neuro-inflammation and deregulation of iron homeostasis in the neurovascular unit (neuron, black; astrocyte, blue; and vasculature, red border) of the ischemic brain. The gene symbols with red color were identified in our experiment, whereas the one with bold red had at least one of the quantification ratio with a significant *p*-value. Multiple cell-specific roles of Glu in the form of a neurotransmitter, metabolic intermediate and as a signaling molecule are shown that acted as a connecting link between the Glu excitotoxicity and the altered energy metabolism. Up-regulation of ubiquitous Glud1 would help in this neurometabolic coupling. Both Glul and Pygb have predominantly an astrocytic localization. Pygb would complement the anaerobic glycolysis under ischemic conditions by utilizing the stored glycogen in the astrocytes. Astrocytic Glu uptake through up-regulated transporters (e.g., Slc1a3, Slc1a2) is coupled with an increased Na^+-driven glucose uptake stimulating the glycolysis in astrocytes during early reperfusion. In the vessel lumen, vascular dysfunction and reactive oxygen species (ROS) induced hemolysis would produce serum free hemoglobin (Hbb), heme and iron. Hemopexin (Hpx) and ceruloplasmin (Cp) - Tf system would act to keep free heme or iron within normal limits. Vascular dysfunction and free radical-mediated leakage of BBB would cause the accumulation of several circulatory proteins (e.g., Tf, Cp, Hpx, Hbb, and Alb) inside the brain parenchyma with an increasing presence until 24 h of I/R injury. ETC is electron transport chain; Hk1 is hexokinase-1; Glc-6-P is glucose-6-phosphate; α-KG is α-keto glutarate; TCA is tricarboxylic acid.

cleft is quickly taken up by the specific high-affinity excitatory amino acid transporters (mainly Slc1a3 and Slc1a2) under physiological conditions to prevent overstimulation of the neuronal Glu receptors (Figure 8). Their predominant astrocytic localization justifies the significant up-regulation (Table 3, Figure 6B) following 4 h of reperfusion as seen with cultured astrocytes upon Glu exposure.[46] Additionally, the up-regulation of ubiquitous Glud1 in astrocytes would complement this Glu uptake by using the neurotransmitter as an energy substrate to replenish α-keto glutarate along with NH_4^+ to sustain the TCA cycle. Immunoreactivity of Glud1 in the astrocytic processes surrounding the glutaminergic nerve endings had been observed providing indirect evidence to the above event.[47] Depletion of the negative regulator, GTP or increase in the positive regulator, ADP under ischemic conditions will promote the ammoniagenesis through the forward reaction by Glud1, having a pH-stabilizing effect on the lactic acidosis, the well-known early event in the pathophysiological cascade of stroke. Increased catabolism of Glu by stabilization of Glud1 mRNA in the rat kidney following metabolic acidosis[48] or its up-regulation both at the mRNA and protein levels in the rat brain neuroblastoma cell line under conditions of simulated hypoxia or ischemia[21] was suggestive of the above phenomenon.

It is conceivable that acute shortage of blood-borne glucose and oxygen following 2 h of ischemia will shift the brain energy metabolism from an aerobic to an anaerobic mode with active participation of astrocytes due to their ability to use stored glycogen. The brain-specific isoform of glycogen phosphorylase, Pygb with its predominant astrocytic localization will supplement glucose-6-phosphate from glycogen and can further save one mole of ATP thus making it an attractive substrate under ischemic conditions.[49] Predictably, a glycogenolysis-mediated rapid decrease in brain glycogen level has been observed in a model of *in vitro* ischemia using a guinea pig hippocampal slice culture.[50] Hence, a concomitant up-regulation of Pygb and several glycolytic enzymes (Tpi1, Pgam1, Pgk1) after 2 h of MCAO (Figure 6A) indicated for the first time an increased mobilization of astrocytic glycogen in an ischemic brain. The relative decrease of all regulated glycolytic enzymes along with Pygb after 4 h of reperfusion compared to 2 h of ischemia

dx.doi.org/10.1021/pr200673y |*J. Proteome Res.* 2011, 10, 5199–5213

(Table 3) was attributed to the blood supply induced restoration of glucose-driven aerobic metabolism in most parts of the ischemic territory causing a compensatory decrease on glycogen dependency. Therefore, detailed understanding of these astrocyte-mediated survival responses could provide important insights about the evolution of cerebral I/R injury and metabolically targeted stroke therapeutics.

Neuro-inflammation and Failure of Iron Homeostasis

Our study provided an evidence that breakdown of the BBB starts in parallel with the early events like failure of the energy metabolism or Glu excitotoxicity and precedes serious tissue damage.[40] This hyper-acute opening of the BBB may cause a leakage of the brain-specific proteins to the circulation that could be potential serum-specific prognostic biomarkers for predicting the therapeutic outcome or progression of the disease. Reportage of many brain specific proteins from our data set as potential serum biomarkers for stroke (Gfap, Uchl1, S100b)[51,52] is consistent with the above hypothesis. Conversely, concentration of the extravasated acute phase proteins in the circulation may be reduced as seen for Tf in stroke patients,[15] or synthesis by the target organ (e.g., liver) may be increased as a part of a compensatory response to provide surrogate markers for stroke. Nonetheless, some of the novel candidates (Pzp or Mug1) from this group (Table 3) may be useful for prospective validation studies to improve the sensitivity or specificity of the commonly used predictors of long-term mortality after acute ischemic stroke. Thus, tissue-based proteomics profiling may be a complementary strategy for the discovery of stroke-biomarkers due to the presence of a permeable BBB.

Peaking of Hbb after 2 h of ischemic injury (Table 3) was contributed by the serum-free hemoglobin originated from the intravascular hemolysis as intact red blood cells (RBC) (diameter: 5 μm) cannot extravasate into brain parenchyma at an early stage.[53] In turn, it reconfirms the leakage of BBB immediately after ischemic injury. Recently free hemoglobin in serum has been found to be associated with atherosclerosis and stroke and proposed as a potential biomarker for ischemic stroke.[54] The reperfusion probably restored the normalcy partly by decreasing the intravascular hemolysis although the leakage of serum-free hemoglobin increased due to progressive opening of BBB. Hence, Hbb was continued to be detected until 24 h postreperfusion with a decreasing magnitude.

Unilateral increase of multiple acute phase proteins (e.g., Tf, Cp, Hpx) (Figure 6C) in the affected hemisphere that are involved in the mobilization of iron to and from the brain cells (transportation and transit from the circulation as well as the intracellular storage), indicated disruption of iron homeostasis during the course of cerebral I/R injury (Figure 8). Recently, Involvement of clathrin has been suggested in Glu excitotoxicity-induced endocytosis following brief episodes of ischemia in the viable neurons.[55] Our study showed increased expression of clathrin in the ischemic hemisphere during excitotoxicity after prolonged I/R injury, indicating the presence of viable and endocytic neurons that can also participate in the uptake of the apo- or holo-Tf following their leakage into the extracellular space.[56] Taken together, hyper-acute yet progressive opening of the BBB with a protein-specific dynamics will have clinical implications not only because of the narrow therapeutic window (i.e., maximum 4.5 h^1) of the sole approved medication (rt-PA) but also the delivery and the pharmacokinetics of prospective drugs in analogous rodent models are critically dependent on the plasma protein binding and permeability of BBB.

Presence of Stroke-Induced Synaptic Plasticity

Increased expression of cell-specific markers (e.g., neuronal Gap43, glial Gfap) indicated activation of specific components of the neurovascular unit (neuron and astrocyte respectively) that constitute the survival response of the I/R injured brain by remodeling and re-establishing new connections. Although Gap43 is predominantly a presynaptic neuron-specific phosphoprotein, a small population of Gfap-positive astrocytes in the cerebrum was found to express this protein following I/R injury in a similar transient MCAO model.[57] Thus, early and sustained up-regulation of Gap43 until 24 h signified a hyper-acute initiation of axonal sprouting and a persistent regeneration of nerves with specific involvement of astrocytes.[58] Up-regulation of Gfap and Vim at 24 h postreperfusion (Table 3) was hallmarks of reactive gliosis in the postischemic brain. These proteins participate in the formation of the intermediate filament network in astrocytes that is a part of the cytoskeleton. The stress induced activation of astrocytes may contribute in the repair or regeneration of the BBB, the neurovascular unit, and the neuron.[59] Thus our study corroborate with others who showed the presence of viable neurons following 24 h or at later time points (48 or 52 h) using imaging techniques.[42] All these proteins may be accounted for the spontaneous recovery in the neurological impairment, observed at 24 h postreperfusion.

Transferrin, a Marker of Neuro-inflammation

The involvement of Tf in the neuro-inflammation and de-regulated iron homeostasis[15] had prompted us to check its spatiotemporal distribution in the affected area of the ipsilateral hemisphere to find the correlation between the Tf level and BBB failure. Our result displayed that the BBB opening is not an all-or-none phenomenon; rather it is a gradual and progressive event. The overlap in the pattern of infarct expansion and Tf presence can potentially make it a marker for BBB breakdown in similar experimental settings to understand the neuro-inflammatory processes.

The other selected candidate, Gfap has a brain-specific origin unlike Tf and has been suggested as a sensitive serum biomarker of brain damage in patients with smaller lacunar lesions or minor strokes[60] or traumatic brain injury.[61] Our study provides unique opportunity to compare the regional and temporal heterogeneity of two potential biomarkers in the ischemic hemisphere having an extra-cranial and brain-specific origin. The reverse expression trends of Tf and Gfap or a pathological increase in the ratio of Tf/Gfap in the Striatum during early reperfusion before the appearance of detectable tissue damage could act as a pathological marker for irreversible brain lesion in the poststroke scenario. Hence, a similar approach can also be adopted for other regulated proteins to generate a pathological fingerprint of specific substructures of the brain to propose event-specific spatiotemporal markers.

Identification of Novel Candidates in Stroke Pathology

A host of proteins never reported in the context of stroke was also regulated during the course of I/R injury (Figure 6D). The down-regulated proteins like, Caskin1 or Epb4.1l1 had direct interaction with a synaptic scaffolding protein, CASK of the membrane-associated guanylate kinase family. Similarly, both Caskin1 and Shank3 were located in the post synaptic density having multidomain scaffolds. Intriguingly, their domain composition was found to be similar amid differences in precise number, type, arrangement and sequence of certain domains. This probably reflects a similar scaffolding function and explains

the concomitant down-regulation in the current model.[62] Thus, parallel down-regulation of all these proteins (e.g., Epb4.1l1, Caskin1 and Shank3) at 24 h post I/R injury is closely associated and may indicate a general decline in the normal synaptic functions. Recently, shank proteins, that organize the Glu receptors at excitatory synapses, were altered in AD-affected brains due to abnormal activity of the ubiquitin-proteosome system (UPS) with Shank3 showing a significant down-regulation.[63] Similar mechanisms can also be implicated in our model as two proteins related to UPS were up-regulated (Uchl1 and Ube1x) indicating its abnormal regulation. Uchl1, a deubiquitinating enzyme present throughout the brain, has also been proposed as a potential biomarker for I/R injury using a 2 h MCAO model.[52]

It is fascinating that many of the regulated synaptic proteins (Mtap6, Apba1, Shank3, and Ctnnd2) have been implicated in chronic neurodegenerative or psychiatric disorders.[64,63,65,66] Mtap6 is a class of microtubule associated calmodulin-binding and calmodulin-regulated protein. Recent studies with Mtap6−/− null mice have indicated that suppression of Mtap6 can cause synaptic defects associated with severe behavioral disorders like schizophrenia.[66] Thus, its significant down-regulation at 4 and 24 h postreperfusion could be related to the compromised state of synaptic plasticity. Hence, further studies are necessary to determine the participation of these proteins in the pathology of stroke-induced motor, cognitive or neuropsychiatric disorders like post-stroke or vascular dementia[67] and stroke-induced depression, anxiety or psychosis, conditions where ischemic stroke acts as a predisposing factor.[68]

CONCLUDING REMARKS

By applying iTRAQ coupled with 2D-LC−MS/MS, we capture for the first time the global-temporal protein expression profile of the affected hemisphere in a validated *in vivo* model of transient focal cerebral ischemia. This regulated list will offer a reference data set for the future studies with analogous rodent or primate models, especially in the absence of a comparable data set from the human ischemic brain samples. It revealed the brain's response to ischemia and reperfusion injury simultaneously to better understand the temporal dynamics of the key facets of stroke pathophysiology unfolding concurrently in an interconnected manner. The detection of several perturbed proteins (Caskin1, Shank3, Kpnb1, Uchl1, Mtap6, Epb4.1l1, Apba1, Ube1x) novel in the context of stroke pathology demonstrated the advantage of this discovery approach. The regulated proteins can be exploited for their validity as serum-specific prognostic biomarkers or pharmacodynamic markers for checking the consequence of drug-target interactions or for reporting the efficacy of the prospective therapeutic candidates on the progression of I/R injury.[1] The detection of system-level emergent properties, like the identification of a metabolic cross-talk between neurons and astrocytes and the breakdown of the BBB in the ischemic brain, is only amenable by an *in vivo* profiling approach. The active involvement of astrocytes as savior of neurons during the acute phase of I/R injury substantiates the changing priorities of stroke research from neuron-specific to cerebro-specific approaches that includes the whole neurovascular unit.[69] BBB damage, despite being reported as a hyperacute event, evolved gradually along with the iron-mediated neurotoxicity, providing a wider therapeutic window. In addition, late recovery or up-regulation of expression of several structural (Myh10, Plec1) and regenerative proteins (Gfap, Vim, Gap43) indicates the presence of putative pleiotropic mechanisms with ample opportunities to promote brain repair by favorably modulating these subacute or chronic events. The phasic response of multiple players during the first 24 h of cerebral I/R injury argues against the conventional approach of sustained and unilateral modulation of certain targets. In turn, the phasic response supports a combination therapy involving multiple targets and addresses the need for careful designing of the therapeutic strategy during future clinical trials depending on the temporal profile of the respective targets. In conclusion, we provide a new strategy in the area of stroke-neuroproteomics for unraveling the hitherto novel molecular mechanisms of cerebral I/R injury.

ASSOCIATED CONTENT

Supporting Information

Supplemental Table 1, Primer sequences of the genes selected for RT-PCR from the regulated list of proteins following iTRAQ experiment. Supplemental Table 2, Summary of the physiological parameters of the four participating Groups in the iTRAQ experiment. Supplemental Table 3A, Complete information of the full list of the qualified proteins (Unused prot sore ≥2, *p*-value <0.05 for at least one ratio) obtained from the bias and background corrected iTRAQ data set. Supplemental Table 3B, Complete information of the proteins included in Table 3 (Result Section) based on their identification information only due to their close association with the regulated proteins. Supplemental Table 4, Pathway Analysis of the regulated and validated proteins from the iTRAQ data set by PANTHER 7.0. Supplemental Figure 1, Changes in physiological variables of Sprague−Dawley rat in MCAO model of cerebral I/R injury and sham group. Supplemental Figure 2, Evolution of cumulative neurological score during the course of cerebral I/R injury. Supplemental Figure 3, TTC staining of representative coronal sections from Sham, 2 + 0 and 2 + 4 group. Supplemental Figure 4, Determination of ratio-specific technical variation using 1166 commonly quantified proteins (unused prot score >2.0) from the three technical replicates. Supplemental Figure 5, Representative RT-PCR images of the temporal regulation of Nefl and Tpm3. Supplemental Data A, Calculation of FDR for each technical replicate and the combined data set. Supplemental Data B, Geometric Mean and Standard Deviation in log space for iTRAQ ratios from three technical replicates. Supplemental Data C, Combined Protein summary from three technical replicates. Supplemental Data D, Combined Peptide summary from the three technical replicates. This material is available free of charge via the Internet at http://pubs.acs.org.

AUTHOR INFORMATION

Corresponding Author

*Correspondence: Siu Kwan SZE, PhD Telephone: (65) 6514-1006. Fax: (65) 6791-3856. E-mail: sksze@ntu.edu.sg.

Author Contributions

†These authors contributed equally to this work

ACKNOWLEDGMENT

We thank Lokesh Bhatt, Prashant Jamadarkhana, Anookh Mohanan, Salil Kumar Bose, Jung Eun Park, Xin Li, Anindya Basu for the experimental assistance and/or critical reading of the

manuscript. The work was supported by grants from the Agency for Science, Technology and Research of Singapore (BMRC: 08/1/22/19/575) and Nanyang Technological University (AcRF: RG 51/10).

REFERENCES

(1) Zaleska, M. M.; Mercado, M. L. T.; Chavez, J.; Feuerstein, G. Z.; Pangalos, M. N.; Wood, A. The development of stroke therapeutics: Promising mechanisms and translational challenges. *Neuropharmacology* **2009**, *56*, 329–41.

(2) Ikonomidou, C.; Turski, L. Why did NMDA receptor antagonists fail clinical trials for stroke and traumatic brain injury? *Lancet Neurol* **2002**, *1* (6), 383–6.

(3) Lo, E. H. A new penumbra: Transitioning from injury into repair after stroke. *Nat. Med.* **2008**, *14* (5), 497–500.

(4) Moskowitz, M. A.; Lo, E. H.; Iadecola, C. The science of stroke: Mechanisms in search of treatments. *Neuron* **2010**, *67* (2), 181–98.

(5) Bayes, A.; Grant, S. G. Neuroproteomics: understanding the molecular organization and complexity of the brain. *Nat. Rev. Neurosci.* **2009**, *10* (9), 635–46.

(6) Luo, Y.; Yin, W.; Signore, A. P.; Zhang, F.; Hong, Z.; Wang, S.; Graham, S. H.; Chen, J. Neuroprotection against focal ischemic brain injury by the peroxisome proliferator-activated receptor-γ agonist rosiglitazone. *J. Neurochem.* **2006**, *97* (2), 435–48.

(7) Sung, J. H.; Cho, E. H.; Kim, M. O.; Koh, P. O. Identification of proteins differentially expressed by melatonin treatment in cerebral ischemic injury - A proteomics approach. *J. Pineal Res.* **2009**, *46* (3), 300–306.

(8) Zhang, Z.; Wu, R.; Li, P.; Liu, F.; Zhang, W.; Zhang, P.; Wang, Y. Baicalin administration is effective in positive regulation of twenty-four ischemia/reperfusion-related proteins identified by a proteomic study. *Neurochem. Int.* **2009**, *54* (8), 488–96.

(9) Dhodda, V. K.; Sailor, K. A.; Bowen, K. K.; Vemuganti, R. Putative endogenous mediators of preconditioning-induced ischemic tolerance in rat brain identified by genomic and proteomic analysis. *J. Neurochem.* **2004**, *89* (1), 73–89.

(10) Cid, C.; Garcia-Bonilla, L.; Camafeita, E.; Burda, J.; Salinas, M.; Alcazar, A. Proteomic characterization of protein phosphatase 1 complexes in ischemia-reperfusion and ischemic tolerance. *Proteomics* **2007**, *7* (17), 3207–18.

(11) Chen, A.; Liao, W. P.; Lu, Q.; Wong, W. S. F.; Wong, P. T. H. Upregulation of dihydropyrimidinase-related protein 2, spectrin α II chain, heat shock cognate protein 70 pseudogene 1 and tropomodulin 2 after focal cerebral ischemia in rats-A proteomics approach. *Neurochem. Int.* **2007**, *50* (7−8), 1078–86.

(12) Carmichael, S. T. Rodent models of focal stroke: Size, mechanism, and purpose. *NeuroRx* **2005**, *2* (3), 396–409.

(13) Fisher, M.; Feuerstein, G.; Howells, D. W.; Hurn, P. D.; Kent, T. A.; Savitz, S. I.; Lo, E. H. Update of the stroke therapy academic industry roundtable preclinical recommendations. *Stroke* **2009**, *40* (6), 2244–50.

(14) Wang, X.; Lo, E. H. Triggers and Mediators of Hemorrhagic Transformation in Cerebral Ischemia. *Mol. Neurobiol.* **2003**, *28* (3), 229–44.

(15) Altamura, C.; Squitti, R.; Pasqualetti, P.; Gaudino, C.; Palazzo, P.; Tibuzzi, F.; Lupoi, D.; Cortesi, M.; Rossini, P. M.; Vernieri, F. Ceruloplasmin/Transferrin system is related to clinical status in acute stroke. *Stroke* **2009**, *40* (4), 1282–8.

(16) Domínguez, C.; Delgado, P.; Vilches, A.; Martín-Gallán, P.; Ribó, M.; Santamarina, E.; Molina, C.; Corbeto, N.; Rodríguez-Sureda, V.; Rosell, A.; Alvarez-Sabín, J.; Montaner, J. Oxidative stress after thrombolysis-induced reperfusion in human stroke. *Stroke* **2010**, *41* (4), 653–60.

(17) Koh, P. O. Proteomic analysis of focal cerebral ischemic injury in male rats. *J. Vet. Med. Sci.* **2010**, *72* (2), 181–5.

(18) Washburn, M. P.; Wolters, D.; Yates, J. R. Large-scale analysis of the yeast proteome by multidimensional protein identification technology. *Nat. Biotechnol.* **2001**, *19* (3), 242–7.

(19) Gygi, S. P.; Rist, B.; Gerber, S. A.; Turecek, F.; Gelb, M. H.; Aebersold, R. Quantitative analysis of complex protein mixtures using isotope-coded affinity tags. *Nat. Biotechnol.* **1999**, *17* (10), 994–9.

(20) Park, J. E.; Tan, H. S.; Datta, A.; Lai, R. C.; Zhang, H.; Meng, W.; Lim, S. K.; Sze, S. K. Hypoxic tumor cell modulates its microenvironment to enhance angiogenic and metastatic potential by secretion of proteins and exosomes. *Mol. Cell. Proteomics* **2010**, *9* (6), 1085–99.

(21) Datta, A.; Park, J. E.; Li, X.; Zhang, H.; Ho, Z. S.; Heese, K.; Lim, S. K.; Tam, J. P.; Sze, S. K. Phenotyping of an in vitro model of ischemic penumbra by iTRAQ-based shotgun quantitative proteomics. *J. Proteome Res.* **2010**, *9* (1), 472–84.

(22) Longa, E. Z.; Weinstein, P. R.; Carlson, S.; Cummins, R. Reversible middle cerebral artery occlusion without craniectomy in rats. *Stroke* **1989**, *20* (1), 84–91.

(23) Belayev, L.; Busto, R.; Zhao, W.; Fernandez, G.; Ginsberg, M. D. Middle cerebral artery occlusion in the mouse by intraluminal suture coated with poly-L-lysine: Neurological and histological validation. *Brain Res.* **1999**, *833* (2), 181–90.

(24) Zausinger, S.; Hungerhuber, E.; Baethmann, A.; Reulen, H. J.; Schmid-Elsaesser, R. Neurological impairment in rats after transient middle cerebral artery occlusion: a comparative study under various treatment paradigms. *Brain Res.* **2000**, *863* (1−2), 94–105.

(25) Joshi, C. N.; Jain, S. K.; Murthy, P. S. R. An optimized triphenyltetrazolium chloride method for identification of cerebral infarcts. *Brain Res. Protoc.* **2004**, *13* (1), 11–7.

(26) Belayev, L.; Alonso, O. F.; Busto, R.; Zhao, W.; Ginsberg, M. D. Middle cerebral artery occlusion in the rat by intraluminal suture: Neurological and pathological evaluation of an improved model. *Stroke* **1996**, *27* (9), 1616–23.

(27) Li, F.; Omae, T.; Fisher, M. Spontaneous hyperthermia and its mechanism in the intraluminal suture middle cerebral artery occlusion model of rats. *Stroke* **1999**, *30* (11), 2464–71.

(28) Chong, P. K.; Gan, C. S.; Pham, T. K.; Wright, P. C. Isobaric tags for relative and absolute quantitation (iTRAQ) reproducibility: Implication of multiple injections. *J. Proteome Res.* **2006**, *5* (5), 1232–40.

(29) Kersey, P. J.; Duarte, J.; Williams, A.; Karavidopoulou, Y.; Birney, E.; Apweiler, R. The International Protein Index: an integrated database for proteomics experiments. *Proteomics* **2004**, *4* (7), 1985–8.

(30) Thomas, P. D.; Campbell, M. J.; Kejariwal, A.; Mi, H.; Karlak, B.; Daverman, R.; Diemer, K.; Muruganujan, A.; Narechania, A. PANTHER: A library of protein families and subfamilies indexed by function. *Genome Res.* **2003**, *13* (9), 2129–41.

(31) del Zoppo, G. J. Microvascular changes during cerebral ischemia and reperfusion. *Cerebrovasc. Brain Metab. Rev.* **1994**, *6* (1), 47–96.

(32) Liu, F.; Schafer, D. P.; McCullough, L. D. TTC, fluoro-Jade B and NeuN staining confirm evolving phases of infarction induced by middle cerebral artery occlusion. *J. Neurosci. Meth.* **2009**, *179* (1), 1–8.

(33) Dittmar, M.; Spruss, T.; Schuierer, G.; Horn, M. External carotid artery territory ischemia impairs outcome in the endovascular filament model of middle cerebral artery occlusion in rats. *Stroke* **2003**, *34* (9), 2252–7.

(34) Zhang, X.; Deguchi, K.; Yamashita, T.; Ohta, Y.; Shang, J.; Tian, F.; Liu, N.; Panin, V. L.; Ikeda, Y.; Matsuura, T.; Abe, K. Temporal and spatial differences of multiple protein expression in the ischemic penumbra after transient MCAO in rats. *Brain Res.* **2010**, *1343* (C), 143–52.

(35) Weinstein, P. R.; Hong, S.; Sharp, F. R. Molecular identification of the ischemic penumbra. *Stroke* **2004**, *35* (11 SUPPL. 1), 2666–70.

(36) Arranz, A. M.; Gottlieb, M.; Perez-Cerda, F.; Matute, C. Increased expression of glutamate transporters in subcortical white matter after transient focal cerebral ischemia. *Neurobiol. Dis.* **2010**, *37* (1), 156–65.

(37) Leiser, S. F.; Kaeberlein, M. A role for SIRT1 in the hypoxic response. *Mol. Cell* **2010**, *38* (6), 779–80.

(38) Haigis, M. C.; Mostoslavsky, R.; Haigis, K. M.; Fahie, K.; Christodoulou, D. C.; Murphy, A.; Valenzuela, D. M.; Yancopoulos, G. D.; Karow, M.; Blander, G.; Wolberger, C.; Prolla, T. A.; Weindruch, R.; Alt, F. W.; Guarente, L. SIRT4 Inhibits Glutamate Dehydrogenase and Opposes the Effects of Calorie Restriction in Pancreatic β Cells. *Cell* **2006**, *126* (5), 941–54.

(39) Yamamoto, H.; Schoonjans, K.; Auwerx, J. Sirtuin functions in health and disease. *Mol. Endocrinol.* **2007**, *21* (8), 1745–55.
(40) Ishii, T.; Asai, T.; Urakami, T.; Oku, N. Accumulation of macromolecules in brain parenchyma in acute phase of cerebral infarction/reperfusion. *Brain Res.* **2010**, *1321* (C), 164–8.
(41) Prajapati, K. D.; Sharma, S. S.; Roy, N. Upregulation of albumin expression in focal ischemic rat brain. *Brain Res.* **2010**, *1327* (C), 118–24.
(42) Wardlaw, J. M. Neuroimaging in acute ischaemic stroke: Insights into unanswered questions of pathophysiology. *J. Intern. Med.* **2010**, *267* (2), 172–90.
(43) Foley, L. M.; Hitchens, T. K.; Barbe, B.; Zhang, F.; Ho, C.; Rao, G. R.; Nemoto, E. M. Quantitative Temporal Profiles of Penumbra and Infarction During Permanent Middle Cerebral Artery Occlusion in Rats. *Transl. Stroke Res.* **2010**, *1* (3), 220–9.
(44) Magistretti, P. J. Role of glutamate in neuron-glia metabolic coupling. *Am. J. Clin. Nutr.* **2009**, *90* (3), 875S–80S.
(45) Bao, X.; Pal, R.; Hascup, K. N.; Wang, Y.; Wang, W. T.; Xu, W.; Hui, D.; Agbas, A.; Wang, X.; Michaelis, M. L.; Choi, I. Y.; Belousov, A. B.; Gerhardt, G. A.; Michaelis, E. K. Transgenic expression of Glud1 (glutamate dehydrogenase 1) in neurons: In vivo model of enhanced glutamate release, altered synaptic plasticity, and selective neuronal vulnerability. *J. Neurosci.* **2009**, *29* (44), 13929–44.
(46) Duan, S.; Anderson, C. M.; Stein, B. A.; Swanson, R. A. Glutamate induces rapid upregulation of astrocyte glutamate transport and cell-surface expression of GLAST. *J. Neurosci.* **1999**, *19* (23), 10193–200.
(47) Aoki, C.; Milner, T. A.; Berger, S. B.; Sheu, K. F. R.; Blass, J. P.; Pickel, V. M. Glial glutamate dehydrogenase: ultrastructural localization and regional distribution in relation to the mitochondrial enzyme, cytochrome oxidase. *J. Neurosci. Res.* **1987**, *18* (2), 305–18.
(48) Schroeder, J. M.; Liu, W.; Curthoys, N. P. pH-responsive stabilization of glutamate dehydrogenase mRNA in LLC-PK_1-F^+ cells. *Am. J. Physiol.: Renal Physiol.* **2003**, *285*, F258–65.
(49) Brown, A. M.; Sickmann, H. M.; Fosgerau, K.; Lund, T. M.; Schousboe, A.; Waagepetersen, H. S.; Ransom, B. R. Astrocyte glycogen metabolism is required for neural activity during aglycemia or intense stimulation in mouse white matter. *J. Neurosci. Res.* **2005**, *79* (1−2), 74–80.
(50) Lipton, P. Regulation of glycogen in the dentate gyrus of the in vitro guinea pig hippocampus; effect of combined deprivation of glucose and oxygen. *J. Neurosci. Meth.* **1989**, *28* (1−2), 147–54.
(51) Whiteley, W.; Chong, W. L.; Sengupta, A.; Sandercock, P. Blood markers for the prognosis of ischemic stroke: A systematic review. *Stroke* **2009**, *40* (5), e380–9.
(52) Liu, M. C.; Akinyi, L.; Scharf, D.; Mo, J.; Larner, S. F.; Muller, U.; Oli, M. W.; Zheng, W.; Kobeissy, F.; Papa, L.; Lu, X. C.; Dave, J. R.; Tortella, F. C.; Hayes, R. L.; Wang, K. K. Ubiquitin C-terminal hydrolase-L1 as a biomarker for ischemic and traumatic brain injury in rats. *Eur. J. Neurosci.* **2010**, *31* (4), 722–32.
(53) Nagaraja, T. N.; Keenan, K. A.; Fenstermacher, J. D.; Knight, R. A. Acute leakage patterns of fluorescent plasma flow markers after transient focal cerebral ischemia suggest large openings in blood-brain barrier. *Microcirculation* **2008**, *15* (1), 1–14.
(54) Huang, P.; Lo, L. H.; Chen, Y. C.; Lin, R. T.; Shiea, J.; Liu, C. K. Serum free hemoglobin as a novel potential biomarker for acute ischemic stroke. *J. Neurol.* **2009**, *256* (4), 625–631.
(55) Vaslin, A.; Puyal, J.; Clarke, P. G. H. Excitotoxicity-Induced Endocytosis Confers Drug Targeting in Cerebral Ischemia. *Ann. Neurol.* **2009**, *65* (3), 337–347.
(56) Horonchik, L.; Wessling-Resnick, M. The Small-Molecule Iron Transport Inhibitor Ferristatin/NSC306711 Promotes Degradation of the Transferrin Receptor. *Chem. Biol.* **2008**, *15* (7), 647–53.
(57) Yamada, K.; Goto, S.; Oyama, T.; Inoue, N.; Nagahiro, S.; Ushio, Y. In vivo induction of the growth associated protein GAP43/B-50 in rat astrocytes following transient middle cerebral artery occlusion. *Acta Neuropathol.* **1994**, *88* (6), 553–7.
(58) Aigner, L.; Arber, S.; Kapfhammer, J. P.; Laux, T.; Schneider, C.; Botteri, F.; Brenner, H. R.; Caroni, P. Overexpression of the neural growth-associated protein GAP-43 induces nerve sprouting in the adult nervous system of transgenic mice. *Cell* **1995**, *83* (2), 269–78.
(59) Pekny, M.; Nilsson, M. Astrocyte activation and reactive gliosis. *GLIA* **2005**, *50* (4), 427–34.
(60) Herrmann, M.; Vos, P.; Wunderlich, M. T.; De Bruijn, C. H. M. M.; Lamers, K. J. B. Release of glial tissue-specific proteins after acute stroke: A comparative analysis of serum concentrations of protein S-100B and glial fibrillary acidic protein. *Stroke* **2000**, *31* (11), 2670–7.
(61) Honda, M.; Tsuruta, R.; Kaneko, T.; Kasaoka, S.; Yagi, T.; Todani, M.; Fujita, M.; Izumi, T.; Maekawa, T. Serum glial fibrillary acidic protein is a highly specific biomarker for traumatic brain injury in humans compared with S-100B and neuron-specific enolase. *J. Trauma: Inj., Infect., Crit. Care* **2010**, *69* (1), 104–9.
(62) Tabuchi, K.; Biederer, T.; Butz, S.; Südhof, T. C. CASK Participates in Alternative Tripartite Complexes in which Mint 1 Competes for Binding with Caskin 1, a Novel CASK-Binding Protein. *J. Neurosci.* **2002**, *22* (11), 4264–73.
(63) Gong, Y.; Lippa, C. F.; Zhu, J.; Lin, Q.; Rosso, A. L. Disruption of glutamate receptors at Shank-postsynaptic platform in Alzheimer's disease. *Brain Res.* **2009**, *1292* (C), 191–8.
(64) Swistowski, A.; Zhang, Q.; Orcholski, M. E.; Crippen, D.; Vitelli, C.; Kurakin, A.; Bredesen, D. E. Novel mediators of amyloid precursor protein signaling. *J. Neurosci.* **2009**, *29* (50), 15703–12.
(65) Arikkath, J.; Peng, I.; Ng, Y. G.; Israely, I.; Liu, X.; Ullian, E. M.; Reichardt, L. F. Delta-catenin regulates spine and synapse morphogenesis and function in hippocampal neurons during development. *J. Neurosci.* **2009**, *29* (17), 5435–42.
(66) Bosc, C.; Andrieux, A.; Job, D. STOP Proteins. *Biochemistry* **2003**, *42* (42), 12125–32.
(67) Pendlebury, S. T. Stroke-related dementia: Rates, risk factors and implications for future research. *Maturitas* **2009**, *64* (3), 165–71.
(68) Chemerinski, E.; Levine, S. R. Neuropsychiatric disorders following vascular brain injury. *Mt. Sinai J. Med.* **2006**, *73* (7), 1006–14.
(69) Lo, E. H.; Moskowitz, M. A.; Jacobs, T. P. Exciting, radical, suicidal: How brain cells die after stroke. *Stroke* **2005**, *36* (2), 189–92.